Chapter 6:

Studies of Cobalt Schiff-base Complexes Encapsulated in Zeolite Y and their Catalytic Activity for the Degradation of Rhodamine B

Chapter 6

6.1. INTRODUCTION

Divalent square planar complexes of cobalt with tetra dentate Schiff-bases are most studied transition metal complexes because they have capacity to act as a synthetic oxygen carrier and also provide a range of stable complexes which are considerably important as model systems for oxygen-binding biomolecules.[1, 2] Heterogenization of these homogeneous catalysts could successfully achieved by entrapping these cobalt Schiff-base complexes inside the pores of zeolite Y.[3-5] Interestingly, it has been observed that cobalt salen as a molecular "ship in a bottle" complex can be synthesized in zeolite Y and it can carry oxygen effectively as a cargo with higher stability toward irreversible oxidation than its solution-phase species.[3] Furthermore, remarkable effects of zeolite framework on the magnetic properties and oxygen binding behavior of the complexes are identified.[3] In such a way, encapsulation provides the alternative way to synthesize the stable catalysts which do not degrade, dimerise or deactivate during the catalytic process, because encaged complex are site-isolated, more reactive and selective for the various oxidative organic transformations.[5-16] Recently, these hybrid metal complexes are successfully explored as catalyst for photo-oxidation process for the degradation of dyes with more efficiency than their homogeneous counter parts.[17-19] Dyes with aromatic rings are usually stable and difficult to degrade.[20] The dyes contain color which is most evident indicators of water pollution even at low concentration and these colored effluents can spoil the receiving normal water sources. Therefore it is absolutely necessary to remove or degrade these dyes present in the effluents before discharge into water bodies.[21, 22] Rhodamine B is one of the most important xanthenes dye, which is quite stable and extensively used in textile industry for dyeing different materials like leather, silk, wool and cotton. However, it has harmful effect on exposure and may cause carcinogenic and teratogenic effects on the human health.[23]

In present study, we have synthesized cobalt Schiff-base complexes (CoL1, CoL2, CoL3, CoL4, CoL5, and CoL6) in free state and encapsulated state in zeolite Y and they are employed as catalysts for the degradation of rhodamin B under UV light. The different substituents have been attached to the ligand so that they provide different steric and electronic effects. Larger the group attached, more will be the molecular dimension of the complex. The molecular dimensions of complexes followed the order as CoL1<CoL3<CoL4<CoL5<CoL6, whereas CoL2 complex has comparable end-to-end

distance with CoL1 but it has two bulkier hydroxyl groups on phenyl rings, as a result increase in the molecular dimension of the complex in other direction (Given in Figure 6.1) takes place. Upon encapsulation, consequences of these substituents on the reactivity are investigated by using different characterization tools and catalytic process.

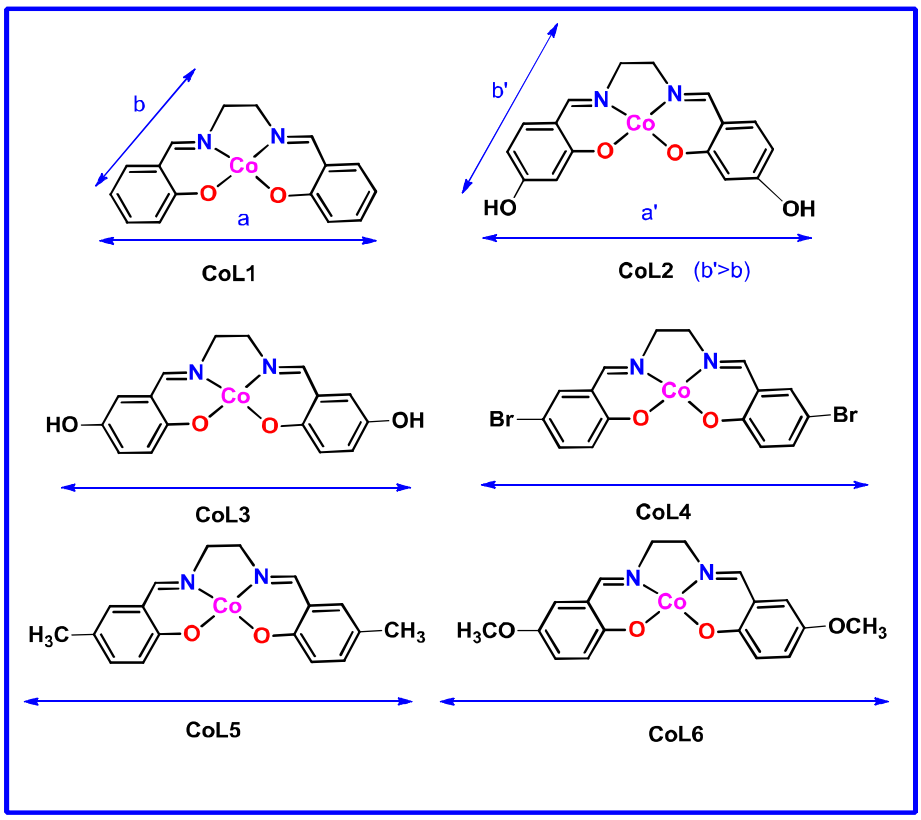

Figure 6.1: Comparative molecular dimensions of cobalt Schiff-base complexes.

These systems are well characterized by powder XRD, SEM-EDS, IR, UV-Visible spectroscopy and magnetic studies. It is quite exciting to compare the photo catalytic activity of the hybrid host-guest systems with their homogeneous counterparts and interestingly reactivity of encapsulated complexes are enhanced and largely controlled by the extent of space constraint imposed by the host framework of zeolite Y.

6.2 RESULTS AND DICUSSION

The synthesis of Schiff-base ligands (L1, L2, L3, L4, L5 and L6), free state cobalt Schiff-base complex (CoL1, CoL2, CoL3, CoL4, CoL5 and CoL6) and degradation of rhodamine B have already been discussed in chapter 2 under experimental section 2.2.1-2.2.6.

6.2.1. Elemental Analysis

The parent Na-zeolite Y has the unit cell formula as $Na_{58}Al_{58}Si_{136}O_{388}{\bullet}yH_2O$ and Si/Al ratio is 2.34. The elemental analysis of hybrid systems of zeolite encapsulated complexes CoL1, CoL2, CoL3, CoL4, CoL5, and CoL6 have indicated that Si/Al ratio remains almost identical with pure zeolite Y suggesting evidently that the encapsulation process doesn't perturb the host framework [EDS spectra are shown in Appendix A43-A49]. The concentration of cobalt metal ion in the Co-exchanged zeolite and encapsulated metal complexes is clearly differentiable, concentration of cobalt metal ions in Co-exchanged zeolite Y is higher than that of the all the zeolite encapsulated complexes. It is quite rational that encapsulation process can induce slight leaching of metal ions which ultimately leads to the little decline of the wt% of cobalt metal in encapsulated complexes.

Table 6.1: Concentration of cobalt (wt %) content in the different samples.

S.No	Samples	Cobalt (wt %)	Si/Al ratio
1.	Parent zeolite Y	-	2.85
2.	Co-Y	1.28	2.90
3.	CoL1-Y	0.35	2.22
4.	CoL2-Y	0.31	2.34
5.	CoL3-Y	0.52	2.48
6.	CoL4-Y	0.37	1.05
7.	CoL5-Y	0.49	2.56
8.	CoL6-Y	0.61	2.18

6.2.2. Scanning Electron Microscopy Analysis

In the present study, encapsulation of metal complex within the supercage of zeolite-Y is essentially targeted inside the cavities of supercage. It's obvious that practically it is not

feasible to control the synthesis procedure in such a way to just implant the complex formation only inside the supercages.

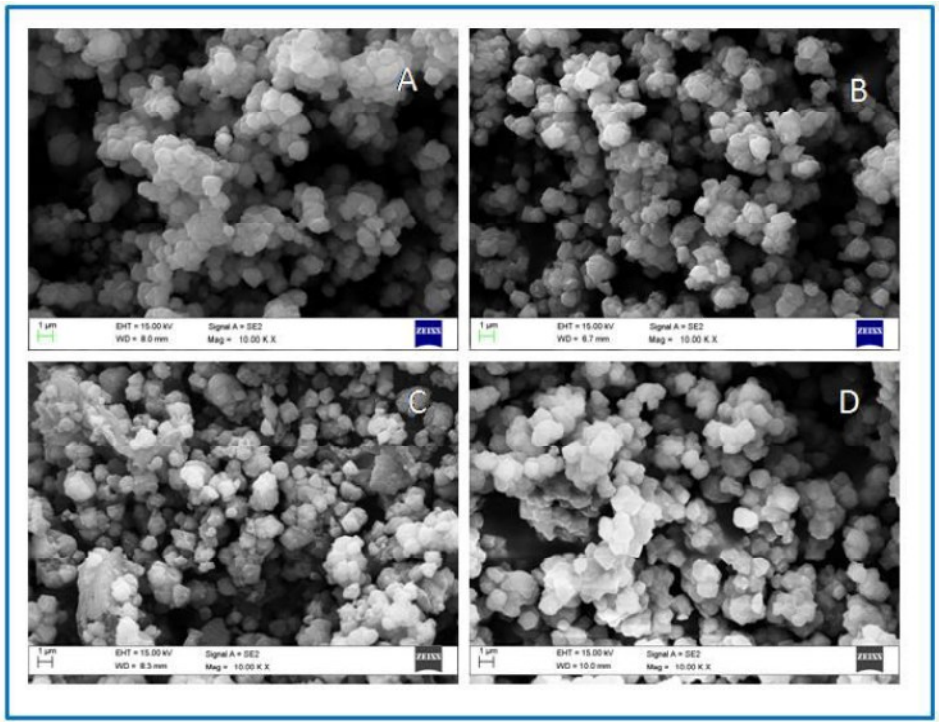

Figure 6.2: SEM images of (A) pure zeolite Y, (B) Co-exchanged-Y, (C) CoL5-Y (before Soxhlet extraction) and (D) CoL5-Y (after Soxhlet extraction).

Therefore formation of the complex on the surface of zeolite and even adsorption of ligand on the surface are practically inevitable. However the complexes formed and ligand adsorbed on the surface of zeolite lattice have been removed by extensive Soxhlet extraction so that to attain the maximum possible concentration of complexes inside the cavities.SE micrographs of pure zeolite Y and encapsulated complexes are recorded (Figure 6.2). It is obvious that after Soxhlet extraction, surface boundaries of host lattice are differentiable and clearly visible. These images are practically presenting the sign of the removal of surface impurities from the host lattice. Additionally, preservation of crystallinity of zeolite framework also can be explicable from SE images.[24, 25]

6.2.3. Powder X-ray Diffraction Analysis

Powder X-ray diffraction patterns of pure zeolite Y, Co-exchanged zeolite Y and zeolite samples with cobalt Schiff-base complexes encapsulated have been recorded (presented in

Figure 6.3). Comparative X-ray diffraction patterns of pure and Co-exchanged zeolite Y and encapsulated cobalt Schiff-base complexes (CoL1-Y, CoL2-Y, CoL3-Y, CoL4-Y, CoL5-Y and CoL6-Y) are essentially similar in terms of peak positions. This observation undeniably specifies the conservation of host lattice integrity during and after the encapsulation process of a large complex into it. Whereas, XRD patterns of encapsulated complexes (CoL1-Y, CoL2-Y, CoL3-Y, CoL4-Y, CoL5-Y and CoL6-Y) have shown considerable reversal in the intensity of the peaks at $2\theta=10°$ and 12° i.e., ($I_{220} < I_{311}$) in contrast to that in the XRD patterns of pure and Co-exchanged zeolite Y. The observed intensity reversal has already been explored and also empirically correlated with presence of large molecule or complex inside the supercage of zeolite Y.[26, 27] Such reversal in the intensity in the mentioned peak is not observed if a complex is tethered on the host surface.[28]

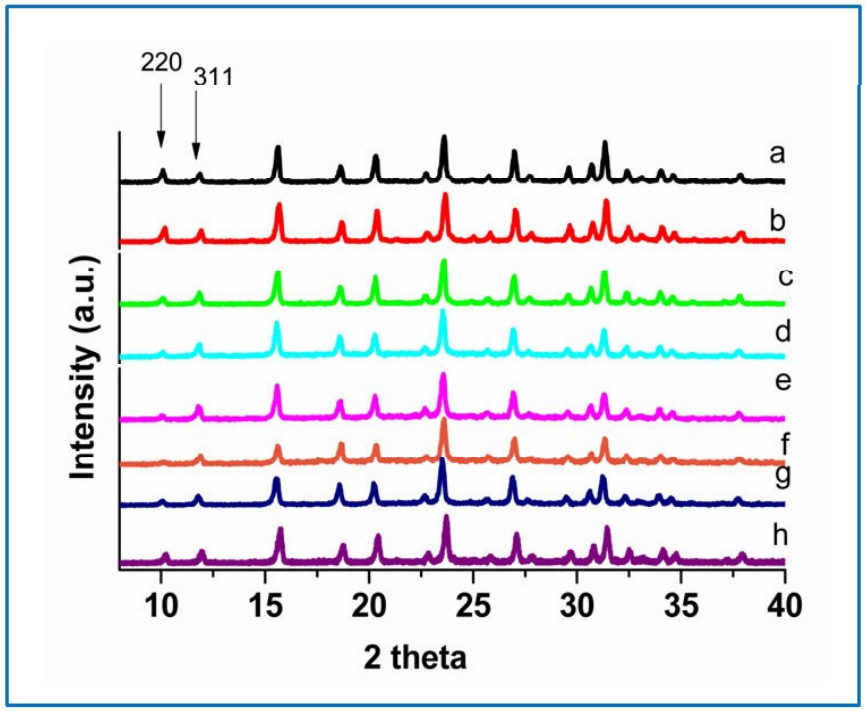

Figure 6.3: XRD pattern of (a) Pure zeolite-Y, (b) Co-exchanged zeolite -Y,(c)CoL1-Y, (d) CoL2-Y, (e) CoL3-Y, (f) CoL4-Y, (g) CoL5-Y and (h) CoL6-Y

Furthermore, the absence of new peaks in XRD patterns of cobalt encapsulated complexes is indeed sign of formation of the complexes in low concentrations as well as inside the host lattice.

6.2.4. IR Spectroscopy

FT-IR spectral data of free state as well as encapsulated cobalt Schiff-base complexes (CoL1-Y, CoL2-Y, CoL3-Y, CoL4-Y, CoL5-Y and CoL6-Y) are recorded (Given in Table 6.2 and Figures 6.4-6.5). Along with the information about the preservation of zeolite Y framework during the process of encapsulation, comparative IR data of pure zeolite Y with cobalt salen complexes encapsulated in zeolite Y have provided information about the successful complex formation within the supercage of zeolite Y as well.

Table 6.2: FTIR spectral data (in cm^{-1}) for neat and encapsulated cobalt Schiff-base complexes.

S.No	Samples	C=N stretching	C=C stretching	ν_{C-H} deformation	C-O stretching
1.	L1	1633	1557,1488	1374	1286
2.	CoL1	1625	1528,1447	1346	1228
3.	CoL1-Y	1630	1445	1359	1219
4.	L2	1643	1586, 1470	1356	1284
5.	CoL2	1604	1534,1442	1386	1282
6.	CoL2-Y	1606	1546,1450	1350	1219
13.	L3	1639	1508,1454	1385	1257
14.	CoL3	1627	1556,1443	1387	1220
15.	CoL3-Y	1646	1547,1447	1390	1229
7.	L4	1633	1572, 1481	1390	1361
8.	CoL4	1636	1520,1458	1368	1304
9.	CoL4-Y	1640	1553, 1482	1351	1282
16.	L5	1639	1582,1489	1366	1284
17.	CoL5	1622	1534,1466	1382	1227
18.	CoL5-Y	1647	1553,1467	1387	1230
10.	L6	1639	1589,1494	1325	1272
11.	CoL6	1643	1555, 1475	1383	1226
12.	CoL6-Y	1639	1548,1467	1398	1229

The major characteristics zeolitic IR bands are recorded in the region of (450-1200) cm^{-1} and two additional bands are observed at 1643 cm^{-1} and 3500 cm^{-1}. These IR bands, (560, 717, 786, and 1018 cm^{-1}) are assigned as $(Si/Al\text{-}O)_4$ bending mode, double ring, symmetric stretching and asymmetric stretching vibration respectively,[29] whereas another two IR peaks at 3500 cm^{-1} and 1643 cm^{-1} are attributed to surface hydroxylic group and lattice water molecules respectively.[24] Interestingly, all IR peaks remain unchanged for cobalt Schiff-base encapsulated systems (CoL1-Y, CoL2-Y, CoL3-Y, CoL4-Y, CoL5-Y and CoL6-Y) specify that the zeolite framework doesn't undergo any structural modifications during the encapsulation process. With the help of IR spectroscopic information of ligands and 'free state' complexes are also proved.

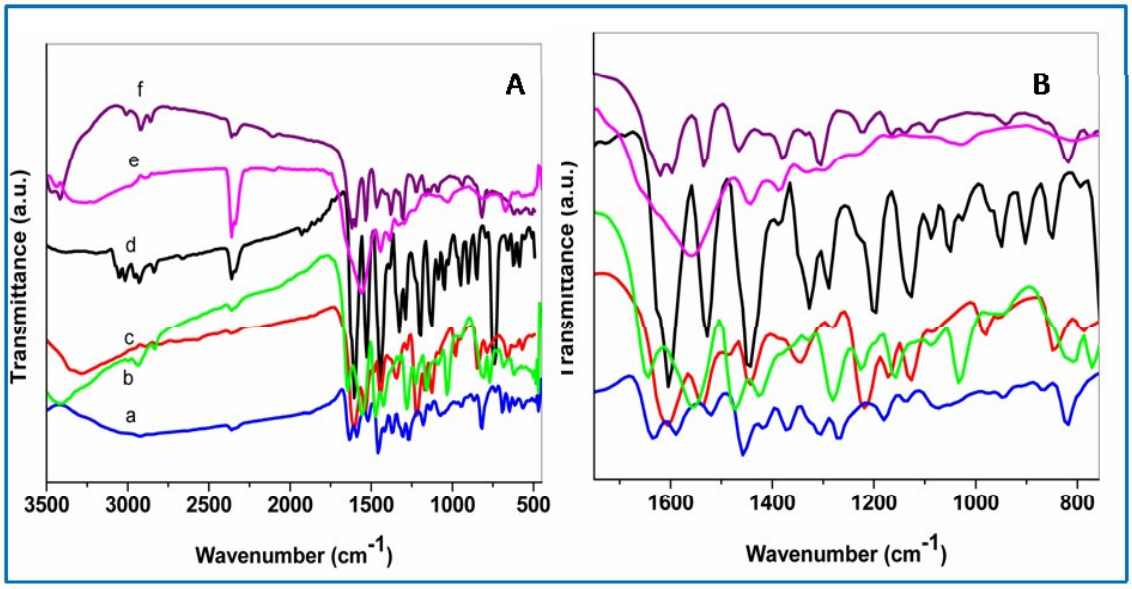

Figure 6.4: (A)FTIR spectral data of cobalt Schiff-base complex in free state (a) CoL4, (b) CoL6, (c) CoL2, (d) CoL1, (e) CoL3 and (f) CoL5.(B) Enlarged view of in the range 1700- 800 cm^{-1} of cobalt Schiff-base complex in free state.

The informative IR peaks of salen ligands as C=N stretching, C=C stretching and C-O stretching vibrations have been identified and they appear at the expected positions. In the Schiff-base complexes these IR bands have appeared at essentially identical positions with marginal shifts towards lower energies because of the coordination with the metal ion. Unfortunately, the IR peaks of the encapsulated complexes are difficult to identify with clarity, as the strong zeolitic bands have appeared in entire (450–3500) cm^{-1} region.

Beneficially, some characteristics IR peaks of encapsulated complexes are observed in the range of (1600-1200) cm^{-1} since zeolitic IR bands are silent in this region.

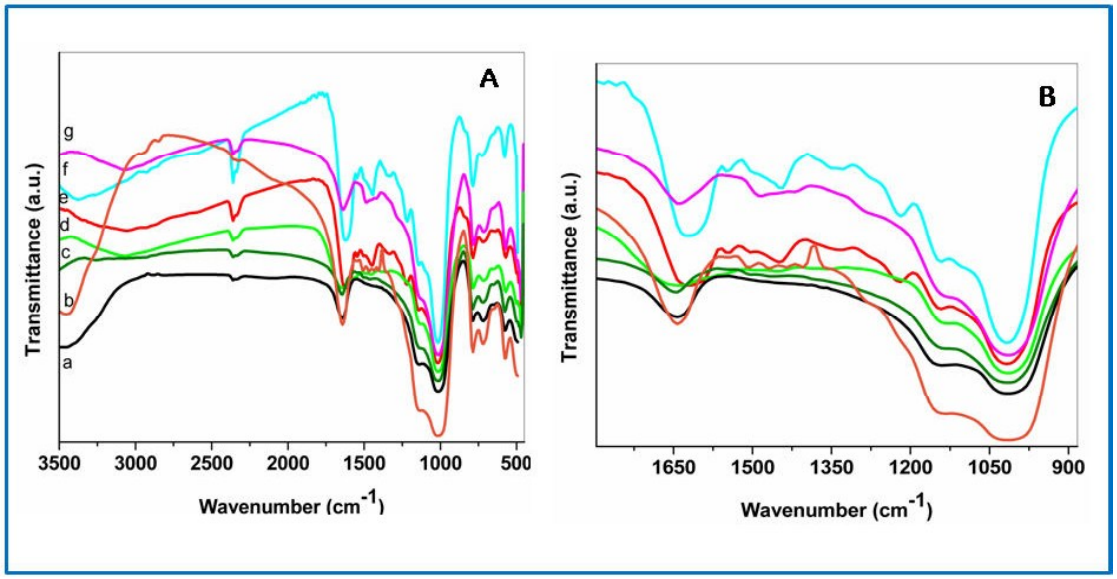

Figure 6.5:(A) FTIR spectral data of cobalt Schiff-base complex in free state (a) pure zeolite Y, (b) CoL6-Y, (c) CoL5-Y, (d) CoL3-Y, (e) CoL2-Y and (f) CoL1-Y and (g) CoL4-Y.(B) Enlarged view of in the range 1700- 900 cm^{-1} of cobalt Schiff-base complex in encapsulated state.

These IR bands in encapsulated complexes have appeared with slighter shifts in peak positions with respect to their free state which must be associated with the different environment of the complex around it. The observation about the shift in C-H deformation bands are supported by the previous studies which actually identify the shift in C-H deformation band as sign of the encapsulation of the complex inside the zeolite Y[30, 31]

6.2.5. UV-Visible Spectroscopy

To explore the co-ordination environment and geometries around the metal center of neat and encapsulated complexes, detailed electronic spectroscopic studies are carried out. The comparative UV-Visible spectroscopic studies in solid state of all the cobalt Schiff-base complexes in both states are presented in Figure 6.6, Table 6.3. Electronic spectroscopic data provide the considerable support about the complex formation in the both states. Absorption bands in the range of (246-256) nm are assigned as π-π^* transitions, where as in range of (316-408) nm are primarily attributed to n-π^* transitions.[32]

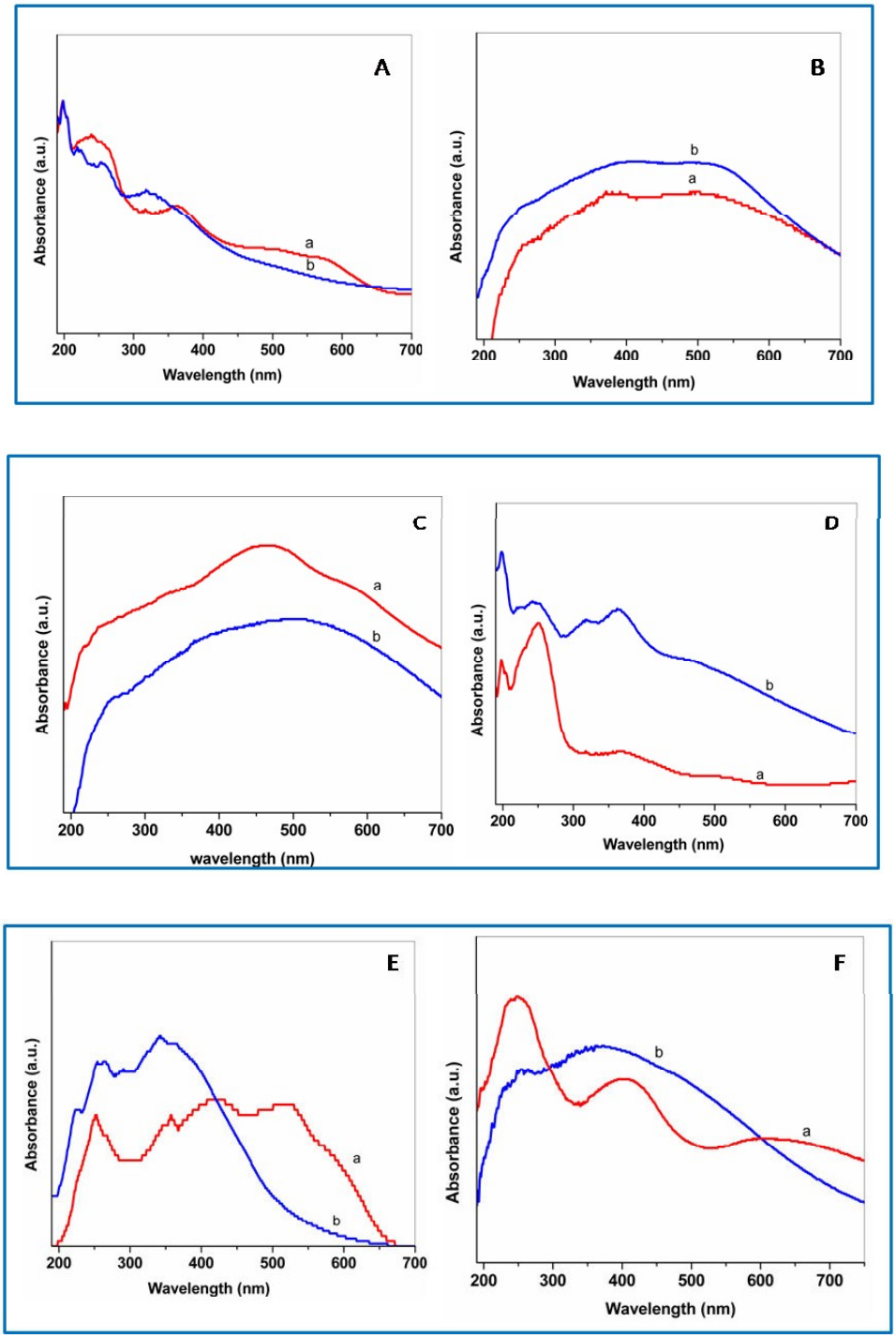

Figure 6.6: Solid state UV-Visible spectra of (A) CoL1 (a), CoL1-Y (b). (B) CoL2 (a), CoL2-Y (b). (C) CoL3 (a), CoL3-Y(b). (D) CoL4 (a), CoL4-Y(b). (E) CoL5 (a), CoL5-Y (b). (F) CoL6 (a), CoL6-Y (b).

The electronic transitions mainly having contribution of d orbitals of metal center are identified comparatively lower energy region of the spectrum. Electronic bands appeared in the range of (401-510) nm and (490-587) nm are recognized to charge transfer (CT) and d-d transitions respectively. UV-Visible data of free CoL1 complex have shown good agreement with the reported data in the literature and indicates the complex formation in the free state.[33, 34] In case of encapsulated complexes, similar prototype of electronic spectra are observed, signifying the complex formation taken place inside the supercage of zeolite Y. Comparative spectroscopic studies of complexes in both the states reveal the fact that intra-ligand transitions (π-π^* and n-π^*) are fairly unaltered under the encapsulation; however transitions involving the metal centers i.e., charge transfer and d-d transitions which are largely affected and have shown the shift peak positions as well as change in intensities for all studied cobalt salen complexes.

Table 6.3: Solid state UV-Visible data (in nm) of cobalt Schiff-base complexes in free and encapsulated state.

S.No	Samples	π—π^* transitions	n—π^* transitions	CT transitions	d-d transitions
1.	CoL1	247	356-370	507	576
2.	CoL1-Y	254	328-340	495	560 (broad)
3.	CoL2	256	316-370	510	573-560 (broad)
4.	CoL2-Y	250	322-368	480	535(broad)
5.	CoL3	250	320-350	Not	585
6.	CoL3-Y	251	325-371	-	545(broad)
7.	CoL4	250	334-368	508	571
8.	CoL4-Y	248	317-365	471	521
9.	CoL5	253	358, 408	519	587
10.	CoL5-Y	251	340, 367	468	510
11.	CoL6	253	350	413	628
12.	CoL6-Y	250	335-336	401	473-492 (broad)

Interestingly, a regular blue shift and intensification of the d-d transitions in the encapsulated cobalt-Schiff-base complexes are observed without any exception. Such behavior already has been observed in the zeolite Y encapsulated complexes and already been reported[30] and also

has been discussed in previous chapters (3A- 3C, 4 and 5). Such modified electronic behavior of electronic spectrum in the d-d region is definitely a consequence of the modified geometry, especially around the metal center of the co-ordination sphere, which is adopted by guest complex under the space restrictions of zeolite framework. Theoretical studies (discussed in previous chapter's 3A-C) have also suggested that changes in different geometrical parameters like the bond angles, bond lengths and HOMO-LUMO gaps are actually initiated in the guest complex by the encapsulation process.

Another exciting observation is that as the complex with larger molecular dimension experiences more steric hindrance with the wall of the host cavity it apparently suffers from more distortion in geometry to minimize the Van der waals interaction with the wall of the supercage. Experimentally, the complex with largest molecular dimensions has shown maximum blue shift in d-d bands in the electronic spectra. In the present work the order of blue shift in d-d region approximately follows the order as CoL6>CoL5>CoL4>CoL3=CoL2>CoL1. This trend is quite rational and can be well correlated with their corresponding molecular dimensions and in turn, extent of distortion. The electronic property of the substituent groups like (-Cl and $-OCH_3$) has quite a prominent impact on the geometry of metal Schiff-base complex.[35, 36] Even the replacement of the atoms in the N_2O_2 square planar proximity by N_2OS and N_2S_2 also leads to the distortion in the geometry of that complex and its consequences can be observed in the electronic behavior of that complex, especially in d-d region.[37]

6.2.6. Magnetic Study

In extension of the electronic study to comprehend the adopted co-ordination environment under encapsulation, FC measurements by using the SQUID magnetometer have been carried out for CoL1, CoL4 and CoL1-Y, CoL4-Y and CoL6-Y (Figure 6.7). Cobalt complexes in neat states are paramagnetic with one unpaired electron. The magnetic moments of the neat complexes fall within the range of 1.92 – 2.52 BM. However under encapsulation, all these complexes have shown distinctly unusual magnetic behavior. as the magnetic behavior of the hybrid systems is originated from the encapsulated complex only as parent zeolite Y is diamagnetic in nature.[27] Cobalt salen complexes apparently adopt non-planar geometry around the metal in the encapsulated state. As a consequence, cobalt ion experiences different electronic environment compared to its free state and compels changes in the ordering of

molecular energy levels. It leads to the drastic change in magnetic behavior with enhanced magnetism of the guest complex compared to its free state.

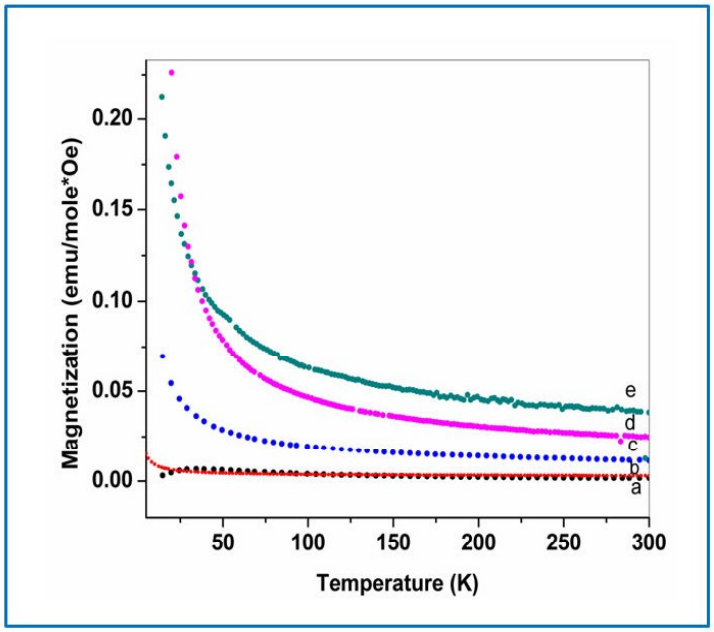

Figure 6.7: Magnetization vs. temperature plots in the range of 5K-300K of the complexes in free and encapsulated states (a) CoL1, (b) CoL4, (c) CoL1-Y (d) CoL6-Y and (e) CoL4-Y.

The comparative molar susceptibility data of CoL1-Y, CoL4-Y and CoL6-Ycomplexes are showing analogous prototype with the observed UV-Visible data as enhanced magnetization is maximum for CoL6-Y than CoL4-Y and then CoL1-Y complexes indicating the largest complex undergo in maximum distortions.

6.2.7. Degradation of Rhodamine B

Photo catalytic degradation of the Rhodamine B (structure shown in Figure 6.7) under ultra violet light has been investigated. Cobalt Schiff base complexes (CoL1, CoL4 and CoL6) in both states have been employed as photo catalyst for the RhB degradation. The degradation reaction is performed in presence of H_2O_2 as oxidant as well as in absence of it (Procedure is already discussed in Chapter 2 under section 2.2.13). The aliquot samples of reaction medium is kept under constant stirring UV light and the monitored at different time intervals at the wavelength of 554 nm (λ_{max} of rhodamine B) by using UV-Visible spectrophotometer and degradation efficiency is calculated with the help of Lambert–Beers law (A= ε.c.l). The

degradation data of RhB are presented in Figures 6.8 and Table 6.4. From the degradation data it is quite clear that the encapsulated complexes are better photo catalysts than their free states and have shown better percentage degradation for RhB in comparison with their homogeneous state. It is also exciting to observe that CoL6 complex has large difference in the photo catalytic activity in encapsulated state than its free state in both cases (with or without H_2O_2). The modified reactivity of CoL6-Y is indeed a consequence of the entrapment of the complex inside the supercage of zeolite-y since the photo catalytic activity of the CoL6 in free state is significantly less than that of even of pure zeolite Y (4.21 %).

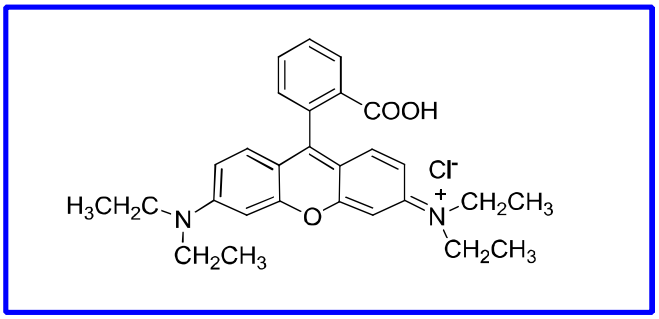

Figure 6.7: Molecular structure of Rhodamine B (RhB)

Table 6.4: The percentage degradation of Rhodamine B in the presence or absence of H_2O_2 under UV light by using cobalt salen complexes as catalysts.

S.No	Samples	RhB degradation without H_2O_2	RhB degradation with H_2O_2
1.	CoL1	4.21	56.73
2.	CoL1-Y	18.18	70.19
3.	CoL4	12.00	99.19
4.	CoL4-Y	25.25	99.45
5.	CoL6	1.00	21.15
6.	CoL6-Y	23.00	89.42

Comparatively lower catalytic activity of the complex in free state might be the outcome of its polymeric nature.[18] While encapsulation process provides the single site isolation of complex and modified geometry. All encapsulated complexes have shown the better activity for the rhodamine B degradation because of their effectiveness for the metal loading, which increases photo generated electron pairs (e^- and h^+). Photo generated holes (h^+) and electrons (e^-) may react with surface hydroxyl groups and can produce the active oxidative ionic radicals(O^{2-}, ^-OOH) and $^{\cdot}OH$) in the presence of water or O_2 from the reaction medium and accelerate the rate of degradation .[18, 38]

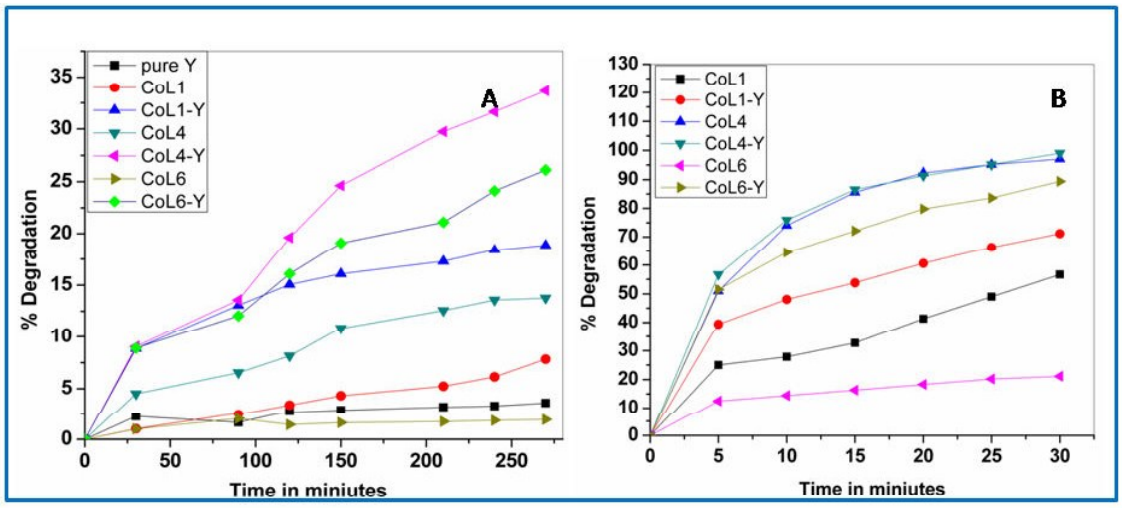

Figure 6.8: The plot between percentage degradation and time taken by the different cobalt Schiff-base complexes in free or encapsulated states under UV light irradiation (A) In absence of hydrogen peroxide (for 270 min) and (B) In presence of hydrogen (for 30 min) peroxide.

6.3 CONCLUSION

Square planar cobalt Schiff-base complexes undergo distortion in geometry after encapsulation in zeolite Y adapted geometry of complex play a decisive role to the modified reactivity of the system. Blue shifted d-d bands in electronic spectra suggest the altering in energy levels of d-orbitals of metal, since the metal center is subjected in the different environment than its free state. Apart from this, the encapsulated complexes have shown better catalytic activity for degradation of rhodamine B since reactivity of the encapsulated complexes is mainly governed by extent of distortion undergone upon encapsulation.

REFERENCES

1. A. Ceulemans, M. Dendooven and L. G. Vanquickenborne, *Inorg. Chem.*, 1985, **24**, 1159-1165.
2. Y. Nishida and S. Kida, *Coord. Chem. Rev.*, 1979, **27**, 275-298.
3. N. Herron, *Inorg. Chem.*, 1986, **25**, 4714-4717.
4. F. Bedioui, E. De Boysson, J. Devynck and K. J. Balkus, *J. Chem. Soc., Faraday Trans.*, 1991, **87**, 3831-3834.
5. C. Jin, W. Fan, Y. Jia, B. Fan, J. Ma and R. Li, *J. Mol. Catal. A: Chem.*, 2006, **249**, 23-30.
6. M. Maurya, S. Titinchi, S. Chand and I. Mishra, *J. Mol. Catal. A: Chem.*, 2002, **180**, 201-209.
7. M. R. Maurya, A. K. Chandrakar and S. Chand, *J. Mol. Catal. A: Chem.*, 2007, **270**, 225-235.
8. M. R. Maurya, A. K. Chandrakar and S. Chand, *J. Mol. Catal. A: Chem.*, 2007, **263**, 227-237.
9. M. R. Maurya, S. J. Titinchi and S. Chand, *J. Mol. Catal. A: Chem.*, 2003, **201**, 119-130.
10. D. Srinivas and S. Sivasanker, *Catal. Surv. Asia*, 2003, **7**, 121-132.
11. R. Raja and P. Ratnasamy, *Catal. Lett.*, 1997, **48**, 1-10.
12. B.-Z. Zhan and X.-Y. Li, *Chem. Commun.*, 1998, DOI: 10.1039/A706030K, 349-350.
13. N. Herron, *J Coord Chem.*, 1988, **19**, 25-38.
14. K. K. Bania and R. C. Deka, *J. Phys. Chem. C*, 2013, **117**, 11663-11678.
15. C. R. Jacob, S. P. Varkey and P. Ratnasamy, *Microporous Mesoporous Mater.*, 1998, **22**, 465-474.
16. J. Dzierzak, M. Lefenfeld and R. Raja, *Top. Catal.*, 2009, **52**, 1669-1676.
17. G. R. Reddy, S. Balasubramanian and K. Chennakesavulu, *RSC Adv.*, 2015, **5**, 81013-81023.
18. G. Ramanjaneya Reddy, S. Balasubramanian and K. Chennakesavulu, *J. Mater. Chem. A*, 2014, **2**, 15598-15610.
19. G. Ramanjaneya Reddy and S. Balasubramanian, *RSC Adv.*, 2015, **5**, 53979-53987.
20. Z. Aksu, *Process Biochem.*, 2005, **40**, 997-1026.

21. G. M. Shaul, T. J. Holdsworth, C. R. Dempsey and K. A. Dostal, *Chemosphere*, 1991, **22**, 107-119.
22. T. Robinson, G. McMullan, R. Marchant and P. Nigam, *Bioresour Technol.*, 2001, **77**, 247-255.
23. V. K. Gupta and Suhas, *J. Environ. Manage.*, 2009, **90**, 2313-2342.
24. K. K. Bania, D. Bharali, B. Viswanathan and R. C. Deka, *Inorg. Chem*, 2012, **51**, 1657-1674.
25. M. Jafarian, M. Rashvand avei, M. Khakali, F. Gobal, S. Rayati and M. G. Mahjani, *J. Phys. Chem. C*, 2012, **116**, 18518-18532.
26. W. H. Quayle, G. Peeters, G. L. De Roy, E. F. Vansant and J. H. Lunsford, *Inorg. Chem*, 1982, **21**, 2226-2231.
27. W. H. Quayle and J. H. Lunsford, *Inorg. Chem.*, 1982, **21**, 97-103.
28. K. K. Bania and R. C. Deka, *J. Phys. Chem. C*, 2012, **116**, 14295-14310.
29. B. Dutta, S. Jana, R. Bera, P. K. Saha and S. Koner, *Appl. Catal., A*, 2007, **318**, 89-94.
30. R. Ganesan and B. Viswanathan, *J. Phys. Chem. B*, 2004, **108**, 7102-7114.
31. A. Choudhary, B. Das and S. Ray, *Dalton Trans.*, 2015, **44**, 3753-3763.
32. A. Böttcher, T. Takeuchi, K. I. Hardcastle, T. J. Meade, H. B. Gray, D. Cwikel, M. Kapon and Z. Dori, *Inorg. Chem.*, 1997, **36**, 2498-2504.
33. P. R. Blum, R. M. C. Wei and S. C. Cummings, *Inorg. Chem.*, 1974, **13**, 450-456.
34. M. Salavati-Niasari, *J. Mol. Catal. A: Chem.*, 2008, **283**, 120-128.
35. M. M. Bhadbhade and D. Srinivas, *Inorg. Chem.*, 1993, **32**, 6122-6130.
36. S. Deshpande, D. Srinivas and P. Ratnasamy, *J. Catal.*, 1999, **188**, 261-269.
37. L. Gomes, E. Pereira and B. de Castro, *Journal of the Chemical Society, Dalton Transactions*, 2000, DOI: 10.1039/A908330H, 1373-1379.
38. G. R. Reddy and S. Balasubramanian, *Microporous Mesoporous Mater.*, 2016, **231**, 207-215.